

# The multikinase inhibitor EC-70124 synergistically increased the antitumor activity of doxorubicin in sarcomas

Oscar Estupiñan<sup>1,2,3</sup>, Laura Santos<sup>1</sup>, Aida Rodriguez<sup>1</sup>, Lucia Fernandez-Nevaldo<sup>1</sup>, Paula Costales<sup>4</sup>, Jhudit Perez-Escuredo<sup>4</sup>, Maria Ana Hermosilla<sup>4</sup>, Patricia Oro<sup>4</sup>, Veronica Rey<sup>1,2</sup>, Juan Tornin<sup>1,2</sup>, Eva Allonca<sup>1</sup>, Maria Teresa Fernandez-Garcia<sup>5</sup>, Carlos Alvarez-Fernandez<sup>6</sup>, Alejandro Braña<sup>7</sup>, Aurora Astudillo<sup>8</sup>, Sofia T Menendez<sup>1,2,3</sup>, Francisco Moris<sup>4</sup> and Rene Rodriguez<sup>1,2,3</sup>

<sup>1</sup>Hospital Universitario Central de Asturias - Instituto de Investigación Sanitaria del Principado de Asturias, Oviedo, Spain

<sup>2</sup>Instituto Universitario de Oncología del Principado de Asturias, Oviedo, Spain

<sup>3</sup>CIBER en oncología (CIBERONC), Madrid, Spain

<sup>4</sup>EntreChem SL, Oviedo, Spain

<sup>5</sup>Unidad Histopatología Molecular en Modelos Animales de Cáncer, IUOPA, Universidad de Oviedo, Oviedo, Spain

<sup>6</sup>Servicio de Oncología Médica of the Hospital Universitario Central de Asturias, Oviedo, Spain

<sup>7</sup>Servicio de Traumatología of the Hospital Universitario Central de Asturias, Oviedo, Spain

<sup>8</sup>Servicio de Anatomía Patológica of the Hospital Universitario Central de Asturias, Oviedo, Spain

Cytotoxic drugs like doxorubicin remain as the most utilized agents in sarcoma treatment. However, advanced sarcomas are often resistant, thus stressing the need for new therapies aimed to overcome this resistance. Multikinase inhibitors provide an efficient way to target several pro-tumorigenic pathways using a single agent and may constitute a valuable strategy in the treatment of sarcomas, which frequently show an aberrant activation of pro-tumoral kinases. Therefore, we studied the antitumor activity of EC-70124, an indolocarbazole analog that have demonstrated a robust ability to inhibit a wide range of pro-survival kinases. Evaluation of the phospho-kinase profile in cell-of-origin sarcoma models and/or sarcoma primary cell lines evidenced that PI3K/AKT/mTOR, JAK/STAT or SRC were among the most highly activated pathways. In striking contrast with the structurally related drug midostaurin, EC-70124 efficiently prevented the phosphorylation of these targets and robustly inhibited proliferation through a mechanism associated to the induction of DNA damage, cell cycle arrest and apoptosis. In addition, EC-70124 was able to partially reduce tumor growth *in vivo*. Importantly, this compound inhibited the expression and activity of ABC efflux pumps involved in drug resistance. In line with this ability, we found that the combined treatment of EC-70124 with doxorubicin resulted in a synergistic cytotoxic effect *in vitro* and an increased antitumor activity of this cytotoxic drug *in vivo*. Altogether, these results uncover the capability of the novel multikinase inhibitor EC-70124 to counteract drug resistance in sarcoma and highlight its therapeutic potential when combined with current treatments.

**Key words:** EC-70124, indolocarbazole, sarcoma, myxoid liposarcoma, doxorubicin, mTOR, ABC pumps, drug resistance

**Abbreviations:** MSC: mesenchymal stromal/stem cells; BMSC: bone marrow-derived mesenchymal stem/stromal cell; ABC: ATP binding cassette; PI3K: phosphatidylinositol-3' kinase; mTOR: mammalian target of rapamycin; MRCLS: myxoid/round cell liposarcoma; FUS: fused in sarcoma; CHOP: C/EBP homologous protein; S6: ribosomal protein S6; 4EBP1: eukaryotic initiation factor 4E-binding protein-1; RTK: receptor tyrosine kinase; IGF1R: insulin-like growth factor I receptor; PDGFR: platelet-derived growth factor receptor; AML: acute myeloid leukemia; H&E: hematoxylin and eosin; FFPE: Formalin-fixed paraffin-embedded; FNCLCC: French Federation of Comprehensive Cancer Centers; CI: combination index; CSC: cancer stem cell

Additional Supporting Information may be found in the online version of this article.

**Conflict of interest:** PC, JP-E, M-AH, PO and FM are employees of EntreChem SL. FM reports ownership of stock in EntreChem SL. All other authors declare they have no competing interests.

**Grant sponsor:** Agencia Estatal de Investigación (Secretaría de Estado de Investigación, Desarrollo e Innovación/Fondo Europeo de Desarrollo Regional (FEDER)); **Grant numbers:** RTC2016-4603-1, SAF-2016-75286-R; **Grant sponsor:** Center for biomedical research network, CIBERONC; **Grant number:** CB16/12/00390; **Grant sponsor:** Fundación para el Fomento en Asturias de la Investigación Científica Aplicada y la Tecnología; **Grant number:** GRUPIN14-003; **Grant sponsor:** Instituto de Salud Carlos III/FEDER (Miguel Servet and Sara Borrell Programs); **Grant numbers:** CPII16/00049, CD16/00103

**DOI:** 10.1002/ijc.32081

**History:** Received 4 Sep 2018; Accepted 5 Dec 2018; Online 21 Dec 2018

**Correspondence to:** Rene Rodriguez, Laboratorio ORL-IUOPA, Hospital Universitario Central de Asturias - Instituto de Investigación Sanitaria del Principado de Asturias, Av. de Roma s/n, 33011 Oviedo, Spain, Tel.: 00-34-985107956, E-mail: renerg.finba@gmail.com or E-mail: rodriguezrene.uo@uniovi.es

**What's new?**

Wide-spectrum multi-kinase inhibitors may help forestall the onset of drug resistance in cancer. In this paper, the authors tested one such inhibitor, called EC-70124, in sarcoma cells. Sarcoma is typically treated with doxorubicin, but advanced sarcomas often develop resistance by way of ABC transporters, which pump the drug out of the cell. Here, the authors showed that EC-70124 not only slowed tumor growth *in vivo*, it inhibited the ABC pumps associated with resistance. EC-70124 also worked synergistically with doxorubicin for increased anti-tumor activity.

**Introduction**

Sarcomas comprise a group of aggressive malignancies which are suggested to develop from transformed mesenchymal stromal/stem cells (MSCs).<sup>1,2</sup> Despite advances in the clinical management of these diseases, the overall survival for patients presenting with metastatic and recurrent disease continues to be dismal<sup>3</sup> and cytotoxic drugs like doxorubicin remain as the mainstay for first-line treatments.<sup>4,5</sup> However, advanced sarcomas often show resistance to doxorubicin, mainly through the overexpression of members of ATP binding cassette (ABC) transmembrane family of transporters which act as efflux pumps for anti-cancer drugs.<sup>6</sup> Therefore, the development of therapeutic strategies able to prevent drug resistance would undoubtedly improve current sarcoma treatments.<sup>7,8</sup>

The phosphatidylinositol-3' kinase (PI3K)/AKT/mammalian target of rapamycin (mTOR) signaling pathway is abnormally activated in many sarcomas and alterations in several components of this axis have been correlated with poor clinical outcome.<sup>9–12</sup> Specifically, myxoid and round cell liposarcomas (MRCLS), an adipocytic tumor characterized by the expression of the fusion oncogene FUS-CHOP, frequently show oncogenic events, such as mutations in *PI3KCA* or overactivation of insulin-like growth factor I receptor (IGF1R) or SRC signaling, which provoke an abnormal activation of these route.<sup>13–18</sup>

mTOR is a serine/threonine protein kinase that exists in two different complexes (mTORC1 and mTORC2). Activated mTORC1 phosphorylates its downstream targets S6 kinase-1, which in turn phosphorylates/activates the ribosomal protein S6 (S6), and the eukaryotic initiation factor 4E-binding protein-1 (4EBP1) resulting in the activation of the synthesis of a panoply of proteins involved in cell growth, metabolism and survival.<sup>11,19</sup> On the other hand, the activation of mTORC2 is involved in actin remodeling and may also contribute to complete activation of mTORC1 through the activation of AKT earlier in the pathway.<sup>9,19</sup> Upstream, the PI3K/AKT/mTOR pathway may be triggered by the activation several receptor tyrosine kinases (RTKs), such as IGF1R, platelet-derived growth factor receptor (PDGFR) or fibroblast growth factor receptor, and nonreceptor tyrosine kinases, like SRC, whose deregulation reportedly plays a role in the tumorigenic process in several types of sarcoma.<sup>15,17,18,20</sup>

Consistent with these findings, the efficiency of several mTOR inhibitors have been evaluated in sarcomas.<sup>9</sup> Clinical testing of rapamycin and its derived analogs has provided at

best only modest results.<sup>21</sup> This limited response may be explained by the fact that these compounds are efficient inhibitors of mTORC1 but not mTORC2 which contribute to induce an adaptive resistance due to the reactivation of AKT.<sup>22</sup> Therefore, a new generation of inhibitors able to target both complexes and/or combinatorial strategies aimed to prevent resistance to mTOR inhibitors are being tested in sarcomas.<sup>22–24</sup>

Targeting several key oncogenic signals with a single agent may constitute an ideal alternative to increase efficiency and prevent the activation of resistance mechanisms. In line with this aim, EC-70124 is a hybrid indolocarbazole analog<sup>25</sup> with a potent multikinase inhibitor spectrum affecting key signaling kinases implicated in pro-survival and proliferative pathways. Thus, EC-70124 have shown antitumor activity in breast, glioblastoma, colorectal and prostate tumors as well as in acute myeloid leukemia (AML) associated to the inhibition of a wide variety of targets including components of the PI3K/AKT/mTOR, JAK/STAT, NFκB or FLT3 pathways.<sup>26–30</sup> Interestingly, midostaurin (PKC-412), an indolocarbazole clinically approved for AML treatment, has shown antitumor activity in certain sarcoma subtypes.<sup>31–33</sup>

Here, we evaluated the antitumor effect properties of EC-70124 and midostaurin in relevant sarcoma models and patient-derived primary cell lines. Opposite to midostaurin, EC-70124 showed strong antiproliferative effects through a mechanism mediated by mTOR inhibition. In addition, this drug inhibited the expression and activity of ABC transporters and synergized *in vitro* and *in vivo* with doxorubicin, thus highlighting the therapeutic potential of this combination.

**Materials and Methods****Cell culture, drugs and ethics statement**

Transformed bone marrow-derived mesenchymal stem/stromal cell (hBMSC) lines with or without expression of FUS-CHOP were previously generated and characterized (Supporting Information Table S1<sup>34,35</sup>). Patient-derived primary cell cultures were generated as described in Supporting Information. An overview of patient and tumor characteristics is given in Supporting Information Table S2. The identity of all cell lines has been authenticated by Short Tandem Repeats analysis during the last 3 months. All the cell lines were tested for Mycoplasma monthly using the LONZA MycoAlert Mycoplasma Detection Kit (LONZA, Rockland CE) and cultured as previously described.<sup>34</sup> EC-70124 was synthesized by a

proprietary process by EntreChem S.L. (Oviedo, Spain). PKC-412 (midostaurin) was synthesized from staurosporine (Biomar Microbial Technologies, León, Spain) and the identity of the isolated product verified by comparison to an authentic sample (High-performance liquid chromatography (HPLC), Nuclear magnetic resonance (NMR)). Stocks of EC-70124, midostaurin, doxorubicin (Sigma, St. Louis, MO), torin, sorafenib, pazopanib, imatinib, BYL-719, BP-1-102 and ruxolitinib (Selleckchem, Houston, TX) were prepared as 10 mM solutions in sterile DMSO for *in vitro* experiments, maintained at  $-20^{\circ}\text{C}$ , and brought to the final concentration just before use. For *in vivo* experiments, doxorubicin was prepared in sterile saline solution and administrated intravenously and EC-70124 was dosed by oral gavage. Human samples and data from donors included in our study were provided by the Principado de Asturias BioBank (PT17/0015/0023) integrated in the Spanish National Biobanks Network. All experimental protocols have been performed in accordance with institutional review board guidelines and were approved by the Institutional Ethics Committee of the Hospital Universitario Central de Asturias.

#### Tumorsphere culture

Tumorsphere formation protocol and the analysis of the effects of drugs on tumorsphere cultures were previously described.<sup>36</sup>

#### Cell viability assays

The viability of all cell lines in the presence and absence of drugs was determined using the Cell Proliferation reagent WST-1 (Roche, Mannheim, Germany) as described before.<sup>37</sup> The concentration of half-maximal inhibition of viability ( $\text{IC}_{50}$ ) for each treatment was determined by nonlinear regression using the graphPad Prism software (La Jolla, CA). The existence of synergy in drug combinations was determined by calculating the combination index (CI) as described in Supporting information.

#### Western blotting and phospho-kinase antibody arrays

Whole cell protein extraction and Western blotting analysis were performed as previously described.<sup>37</sup> Antibodies used are described in Supporting Information.

The phosphorylation status of a wide range of RTKs and downstream signaling nodes was evaluated in EC-70124 or midostaurin-treated cells using the PathScan RTK Signaling Antibody Array Kit (# 7982, Cell Signaling Technology, Danvers, MA). Protein extraction after treatments, array incubation and signal development was performed using the reagents provided by the kit according to the manufacturer's instructions.

Infrared fluorescent signals in Western blotting and antibody array analysis were detected and quantified using Odyssey Fc imaging system and the software Image Studio from LICOR (Lincoln, NE). The signal intensity of the background was subtracted from the signal of each spot, and the average

of duplicate spots was determined. Next, normalized signal intensity was calculated by dividing the mean value in each spot over the mean value in the positive control.

#### Cell cycle analysis

Cell cycle analysis was carried out as described previously.<sup>4</sup>

#### Immunofluorescence staining

In  $\gamma\text{H2AX}$  immunofluorescence experiments, fixation, staining and mounting of the samples were performed as previously reported.<sup>4</sup> Antibodies and experimental conditions are described in Supporting Information.

#### RT-qPCR assays

The expression of ABCB1 and ABCG2 was assessed by qPCR as described in Supporting Information.

#### Transporter substrate and inhibition assays

The assessment of the ability of EC-70124 to inhibit ACBB1/MDR1 and ABCG2/BCRP1 or to be a substrate for these transporters were performed by Absorption Systems (Exton, PA) as described in Supporting Information.

#### *In vivo* tumor growth

All experimental protocols were carried out in accordance with the institutional guidelines of the University of Oviedo and were approved by the Animal Research Ethical Committee of the University of Oviedo prior to the study. Female NOD/SCID mice of 6 weeks old (Janvier Labs, St. Berthevin, France) were inoculated subcutaneously (s.c.) with  $2 \times 10^6$  T5H-FC#1 cells. Once tumors reached 200–300 mm<sup>3</sup>, the mice were randomly assigned to receive vehicle, EC-70124 (80 mg/Kg, q2dx11, orally), doxorubicin (4 mg/Kg, q4dx3, intravenous) or the combination of EC-70124 (40 mg/Kg, q2dx8, orally) and doxorubicin (4 mg/Kg, q4dx3, intravenous), intravenous. Animals were sacrificed by CO<sub>2</sub> asphyxiation when tumors of the control series reached approximately 1,000 mm<sup>3</sup> or if severe weight loss were observed. Mean tumor volume differences between groups were determined using a caliper (Supporting Information). The student *t* test was performed to determine the statistical significance between different groups. The *F* test was used to compare tumor volume growth kinetics. Drug efficacy was expressed as the percentage tumor growth inhibition (%TGI; Supporting Information). For pharmacodynamic studies, a single dose of each treatment was inoculated into immunodeficient mice carrying tumors of approximately 400–500 mm<sup>3</sup>. Tumors ( $n = 2/3$  per group) were collected after 4, 24 or 48 hr, minced, washed with PBS and homogenized in ice-cold lysis buffer (1 ml/100 mg of tumor; see Supporting Information for buffer composition) using a GentleMACS Dissociator system (Miltenyi Biotec, Bergisch Gladbach, Germany) according to manufacturer instructions. This homogenate was centrifuged at 10,000g for 20 min at 4°C, and the supernatants containing

protein extracts were transferred to new tubes and used in Western blotting experiments.

### Histological analysis

Tumor samples were fixed in formol, embedded in paraffin, cut into 4- $\mu$ m sections and stained with hematoxylin and eosin (H&E). Tumor sections were also subjected to immunohistochemistry as previously reported<sup>38</sup> using the antibodies and quantification methods described in Supporting Information. Tumor grade was analyzed in H&E stained preparations using the French Federation of Comprehensive Cancer Centers (FNCLCC) grading system (Supporting Information).

## Results

### Differential effects of the indolocarbazole analogs EC-70124 and midostaurin in sarcoma

To study the antitumor effects of indolocarbazole analogs in sarcoma we used previously developed cell-of-origin models of undifferentiated pleomorphic sarcoma (MSC-4H-GFP, MSC-5H-GFP and T-5H-GFP#1) and FUS-CHOP (FC)-expressing MRCLS (MSC-4H-FC, MSC-5H-FC, T-4H-FC#3 and T-5H-FC#1) in which hBMSCs were sequentially mutated with up to six oncogenic events (see Supporting Information Table S1). The evaluation of cell toxicity in dose–response experiments showed that, opposite to wild type hBMSCs, all sarcoma models were sensitive to nanomolar concentrations of EC-70124 (IC<sub>50</sub> values between 180 and 540 nM; Figs. 1*a* and 1*b*). To further characterize the cytotoxic effect of EC-70124, we performed similar dose–response experiments in a panel of primary sarcoma cell lines (described in Supporting Information Table S2). A subgroup of five primary cell lines (CDS1, CDS17, SARC6 and CDS11) show a sensitivity to EC-70124 similar to that observed for the sarcoma models (IC<sub>50</sub> values between 201 and 343 nM), while another three cell lines (SARC1, SARC3 and SARC4) were more resistant (IC<sub>50</sub> values between 705 nM and 1.3  $\mu$ M) (Fig. 1*c*). In accordance with this cytotoxic effect, EC-70124 treatment induced a dose-dependent apoptotic cleavage of PARP both in sarcoma models (MSC-5H-FC and T-5H-FC#1 cells; Fig. 1*d*) and primary cell lines (Fig. 1*e*). In striking contrast to the effect of EC-70124, sarcoma models MSC-5H-FC and T-5H-FC#1 were resistant to the treatment with the structurally related compound midostaurin (Supporting Information Figs. S1A and S1B) and this drug induced only a marginal apoptotic effect compared to that of EC-70124 (Fig. 1*d*). As a control, midostaurin was efficient inhibiting proliferation of a leukemia cell line as previously shown<sup>29</sup> (Supporting Information Fig. S1A). Cell cycle analysis also showed a different response of sarcoma cells to the treatment with both indolocarbazole analogs. Cell cycle profiles of MSC-5H-FC and T-5H-FC#1 cells treated with 1  $\mu$ M EC-70124 were characterized by a strong arrest in S-phase followed by the induction of high levels of apoptosis (Sub-G<sub>1</sub> population). On the other hand, cells treated with 1  $\mu$ M midostaurin quickly arrest in G<sub>2</sub>/M

phase and underwent endoreplication without cell division resulting in cell populations with 8n DNA content after 48 hr of treatment (Fig. 1*f*). In line with the different ability to induce S-phase arrest, EC-70124, but not midostaurin, was able to efficiently induce DNA damage in T-5H-FC cells as indicated by the dose-dependent increase of intranuclear  $\gamma$ H2AX foci levels (Figs. 1*g* and 1*h* and Supporting Information Fig. S2).

Next, we tested the ability of these indolocarbazole analogs to target cancer stem cell (CSC)-enriched tumorsphere cultures of MSC-5H-FC and T-5H-FC#1 cells.<sup>36</sup> Again, EC-70124 was more efficient than midostaurin in eliminating CSCs (Supporting Information Fig. S1C), although its cytotoxic effect on CSC subpopulations was lower than that previously observed in nonselected adherent cultures (Figs. 1*a* and 1*b*) and also much lower than the effect of the mythramycin analog EC-8042, a drug with reported activity on sarcoma CSCs.<sup>37</sup>

Finally, to compare the cytotoxic effect of EC-70124 with other multikinase inhibitors already approved for cancer treatment, we treated T-5H-FC#1 cells with increasing concentrations of sorafenib, pazopanib and imatinib. All of these drugs were much more inefficient than EC-70124 in reducing cell survival, showing IC<sub>50</sub> concentrations of 20  $\mu$ M or higher (Supporting Information Fig. S3).

### Effect of EC-70124 and midostaurin on the kinase profile of sarcomas

To gain insights about the mechanistic basis of EC-70124-induced cytotoxicity in sarcomas, we used phosphokinase antibody arrays to evaluate the ability of the indolocarbazole analogs to inhibit the phosphorylation/activation of 39 relevant receptor tyrosine kinases and signaling transducers. In T-5H-FC#1 cells, EC-70124 induced an efficient and durable inhibition of several components of the PI3K/AKT/mTOR and MAPK pathways, including phospho-AKT (T308 and S473), phospho-S6 (S235/236) and phospho-ERK1/2 (T202/Y204; Figs. 2*a* and 2*b*, Supporting Information Figs. S4A and S5). On the other hand, midostaurin produced a much reduced and reversible inhibition of these targets (Figs. 2*a* and 2*b*). Western blotting analyses of time-course (Fig. 2*c*) and dose–response experiments (Fig. 2*d*) confirmed that EC-70124 is much more efficient than midostaurin in inhibiting the phosphorylation of AKT and the mTOR downstream targets S6 and 4EBP1 in MRCLS models, without affecting total protein levels. Complementary, we calculated the inhibitor binding constants (K<sub>d</sub> values) for a panel of kinases in the presence of several concentrations of EC-70124 or midostaurin (KdeLECT assay, DiscoverX). Similar to that observed measuring phosphorylation levels, EC-70124 showed a higher potency to bind/inhibit mTOR signaling (S6K1, RSK2, RSK3 and RSK4) and cell cycle-related kinases (CHK1, AURKA, AURKB and AURKC; Supporting Information Table S3).

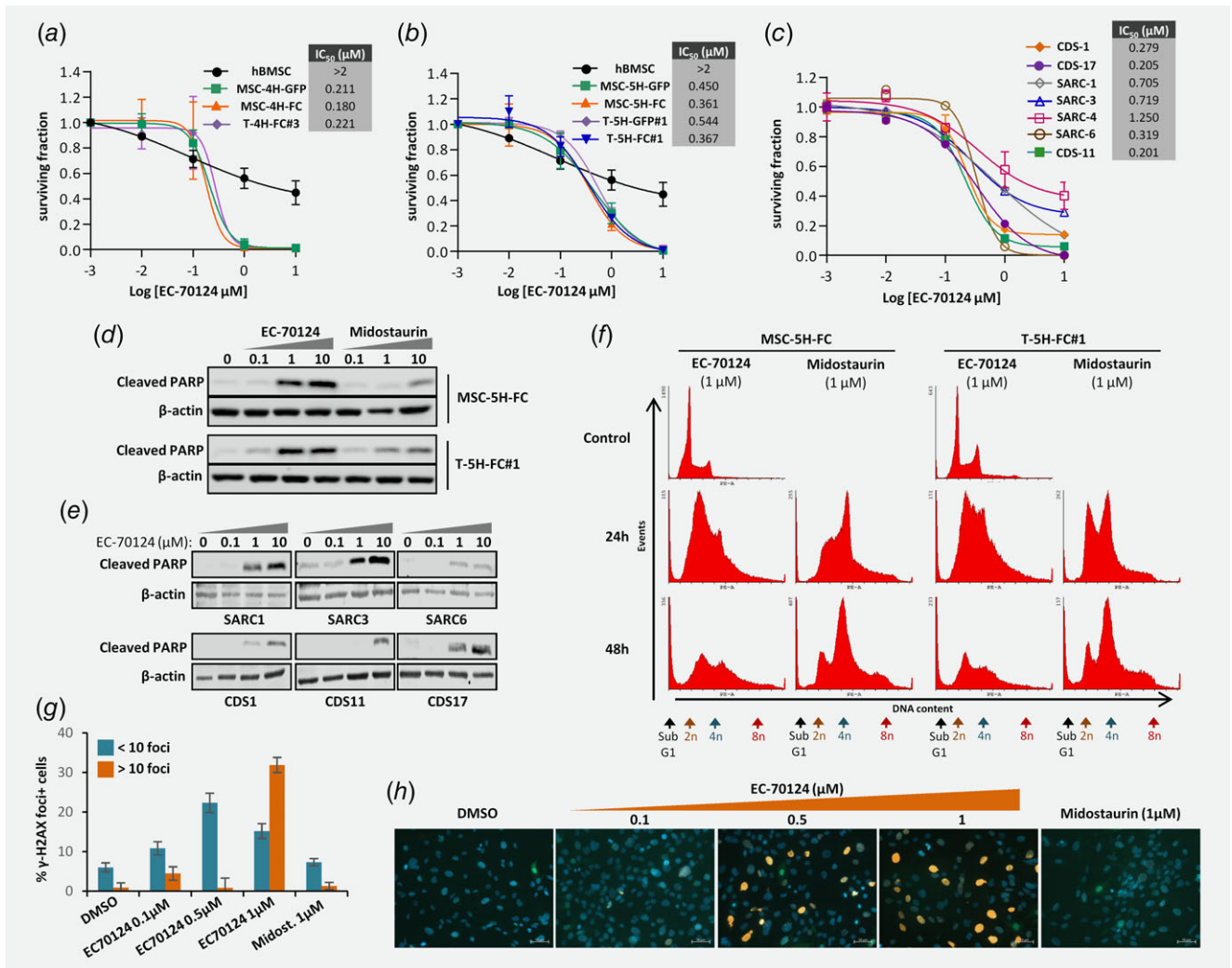


**Figure 1.** Antiproliferative effects of EC-70124 and midostaurin in sarcoma. (a–c) Cell viability (WST1 assay) measured after the treatment of wild-type hMSCs and the indicated MSC-4H, T-4H (a), MSC-5H and T-5H cells lines (b) or several patient-derived sarcoma primary lines (c) with increasing concentrations of EC-70124 for 48 hr.  $IC_{50}$  values for each cell type are shown. Error bars represent the standard deviation of at least three independent experiments. (d and e) Apoptotic cleavage of PARP in MSC-5H-FC and T-5H-FC#1 cells (d) or several primary cell lines (e) treated with the indicated concentrations of EC-70124 or midostaurin for 24 hr. The expression of  $\beta$ -actin was used as loading control in Western blotting analysis. (f) Time-course evolution of the cell cycle distribution of MSC-5H-GFP and MSC-5H-FC cells treated with 1  $\mu$ M EC-70124 or midostaurin. Peaks of cell populations with 2n, 4n and 8n DNA content, as well as the SubG1 population, are indicated. (g and h) Analysis of  $\gamma$ H2AX foci formation after the treatment of T-5H-FC#1 cells for 6 hr with the indicated concentrations of EC-70124 or midostaurin. (g) Quantification of  $\gamma$ H2AX foci was performed by counting more than 200 cells in each condition. The percentage of cells presenting high (>10 foci) or low level (<10 foci) of DNA damage is displayed. Error bars represent the standard deviation. (h) Representative merged images ( $\gamma$ H2AX immunodetection and DAPI staining) of immunostaining experiments showing a dose-dependent increase in  $\gamma$ H2AX foci formation after EC-70124 treatment. Scale bars = 50  $\mu$ m. A version of this panel showing separate  $\gamma$ H2AX-associated and DAPI fluorescence is displayed as Supporting Information Figure S2. [Color figure can be viewed at wileyonlinelibrary.com]

As in T5H-FC#1 cells, AKT, S6 and ERK1/2 were the kinases/signaling molecules showing a higher level of activation/phosphorylation in three sarcoma primary cell lines. Again, EC-70124 was able to inhibit the phosphorylation of these targets, with the only exception of ERK1/2 in the line CDS1+ and AKT (S473) in the line SARC6+ (Figs. 2e and 2f, Supporting Information Figs. S4C and S5). Of note, the inhibition of phospho-S6 was complete in all the assayed cell lines. In addition, some of the primary cell lines also displayed high levels of phospho-STAT1

(CDS17+ and SARC6+), phospho-STAT3 (CDS1+, CDS17+ and SARC6+) and phospho-SRC (CDS1+ and SARC6+) and EC-70124 efficiently inhibited these phosphorylations (Figs. 2e and 2f). In Western blotting analysis of dose–response experiments, we confirmed the ability of EC-70124 to inhibit the phosphorylation of phospho-AKT, phospho-S6 and phospho-STAT3 in six primary cell lines (Fig. 2g).

Overall, these results indicate that EC-70124 is a more efficient multikinase inhibitor and show a more robust antiproliferative

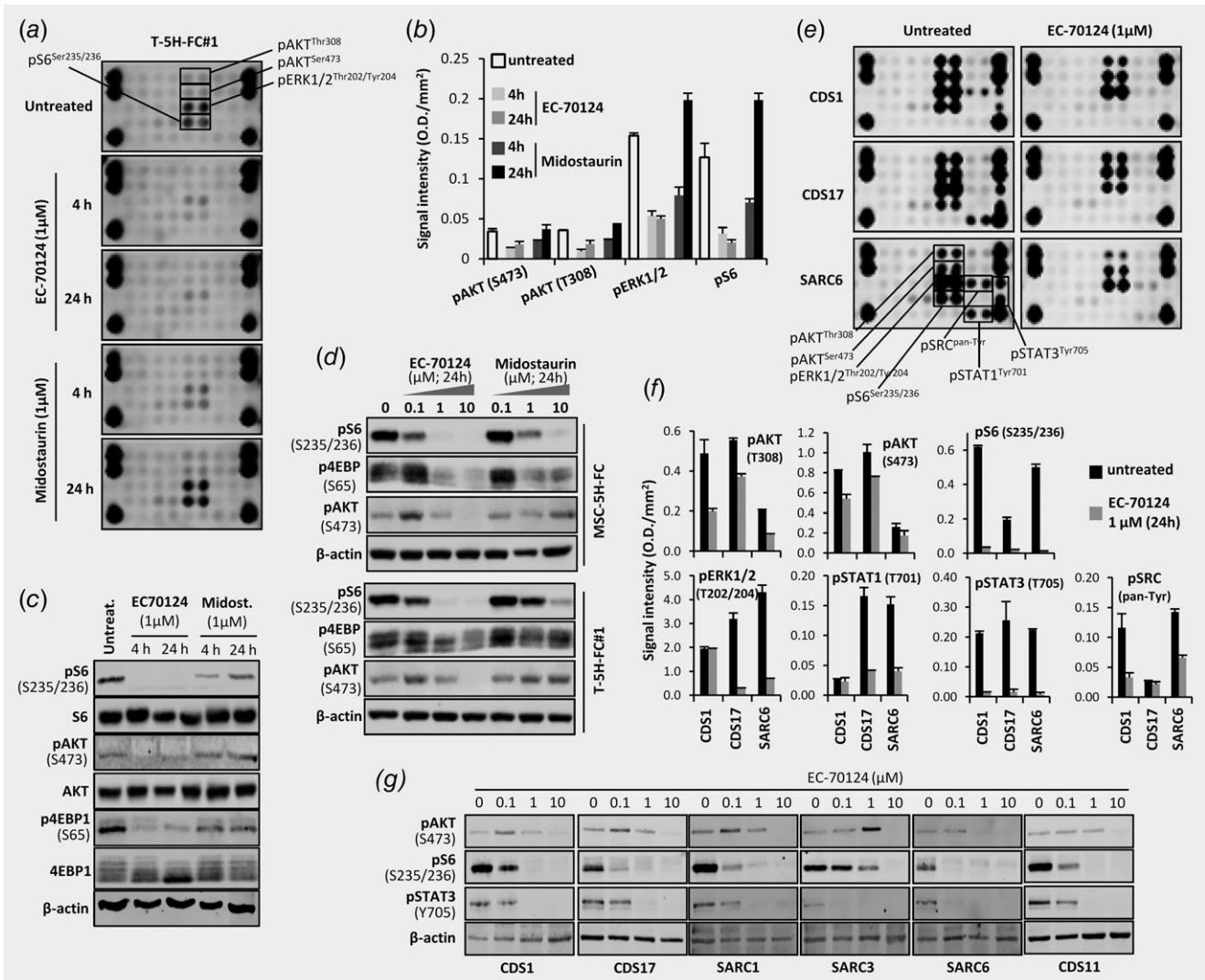


**Figure 2.** Kinase inhibitory profile of EC-70124 and midostaurin. (a and e) Phospho-kinase antibody arrays showing the phosphorylation/activation status of a panel of kinases in T-5H-FC#1 cells after the indicated treatments with EC-70124 or midostaurin (a) or in four primary sarcoma cell lines treated or not with 1 μM EC-70124 for 24 hr (e). (b and f) Quantification of the levels of the indicated phospho-proteins in the kinase arrays loaded with T-5H-FC#1 (b) or sarcoma primary cell lines samples (f). Complete images of the phospho-kinase antibody arrays and the quantification of all analyzed kinases in T-5H-FC#1 and primary cell lines are presented as Supporting Information Figures S3A, S3C and S4, respectively. (c, d and g) Western blotting analysis of the indicated proteins in T-5H-FC#1 cells treated with 1 μM EC-70124 or midostaurin for the indicated times (c), in MSC-5H-FC and T-5H-FC#1 cells treated with the indicated concentrations of EC-70124 for 24 hr (d) and in a panel of primary cell lines treated for 24 hr with the indicated concentrations of EC-70124 (g). Error bars in protein quantifications represent the standard deviation of two duplicates.

effect than midostaurin in sarcomas. Also, they suggest that mTOR signaling inhibition may play a prominent role in EC-70124-induced cytotoxicity.

### mTOR signaling inhibition mediates EC-70124-induced cytotoxicity

To study the relevance of the contribution of mTOR signaling inhibition to the antitumor effects of EC-70124, we analyzed the effects of the well-known mTOR inhibitor torin in T-5H-FC#1 cells. As expected, torin was able to efficiently inhibit

the phosphorylation of AKT, S6 and 4EBP1 (Supporting Information Fig. S6A). We found that, compared to EC-70124 and midostaurin, torin showed an intermediate capacity to reduce cell viability (Supporting Information Fig. S6B), and did not induce DNA damage (Supporting Information Fig. S2). Given that torin is a potent mTOR inhibitor, we hypothesized that if the inhibition of mTOR signaling is involved in the mediation of the cytotoxic effect of EC-70124 we do not expect a great synergy from the combination of this indolocarbazole with torin. Conversely, given that midostaurin is a poor inhibitor

of mTOR signaling, if the inhibition of mTOR signaling is a relevant mechanism we would expect a higher synergistic effect when we combine torin with midostaurin. Investigating this hypothesis, we found that combination of EC-70124 or midostaurin with increasing concentrations of torin enhanced cytotoxicity (Supporting Information Figs. S6C and S6D). However, by representing the data of these combinations normalized to the effect of torin alone, we did not find a relevant shift of toxicity curves in the combinations with EC-70124 (Supporting Information Fig. S6E). Otherwise, we did find an important shift toward higher toxicity in the combinations of torin with midostaurin (Supporting Information Fig. S6F), thus suggesting a more than additive contribution of the mTOR inhibitor to the toxicity of midostaurin. To test whether these combinations has synergistic cytotoxic effect, we calculated their CI using the CompuSyn software. In the case of combinations with EC-70124, we found an intermediate level of synergism (CI value for ED<sub>75</sub> = 0.44) when we assay combinations of drugs that target between 40 and 75% of the cells ( $0.4 < Fa < 0.7$ ). However, this synergistic effect is lost at combinations of higher concentrations of drugs that affect a higher percentage of the cells ( $Fa > 0.8$ ; Supporting Information Fig. S6G). This effect may be explained by the fact that at high concentrations of EC-70124 mTOR signaling is completely inhibited and a mTOR signaling inhibitor like torin cannot add a further effect. On the other hand, and in line with our rationale, the combination of increasing concentrations of torin with midostaurin resulted in a constant increase of the CI, which reached the level of strong synergism when the fraction of cells affected is higher than 70% (CI value for ED<sub>75</sub> = 0.14; Supporting Information Fig. S6G).

To investigate whether the inhibition of other kinases may also play a role in EC-70124 antitumor effect, we tested the effect a PI3K inhibitor (BYL-719), a STAT3 inhibitor (BP-1-102) and a JAK1/2 inhibitor (ruxolitinib) alone or in combinations on T-5H-FC#1 cells. Although at higher concentrations than EC-70124 or torin, BYL-719 was able to inhibit AKT and S6 phosphorylation. In addition, BP-1-102 and ruxolitinib inhibited STAT3 phosphorylation (Supporting Information Fig. S7A). None of these inhibitors were efficient cytotoxic drugs, showing IC<sub>50</sub> concentrations of 20 μM or higher (Supporting Information Figs. S7B–S7D). Moreover, the combination of BP-1-102 with BYL-719 did not produce any increase in cytotoxicity (Supporting Information Fig. S7E).

Altogether, the combination of indolocarbazole analogs with torin suggested that the inhibition of the mTOR signaling plays a relevant role in antiproliferative activity of EC-70124.

#### **In vivo antitumor activity of EC-70124**

Oral treatment of NOD/SCID mice carrying T-5H-FC#1 xenografts with EC-70124 resulted in a moderate tumor growth inhibition. Compared to vehicle treated group, mice treated with 80 mg/Kg of EC-70124 every 2 days showed a percentage of TGI of 26.5% (Fig. 3a). Likewise, at the end of

the experiment, tumor weights of EC-70124-treated mice were significantly lower than those of the control group (Fig. 3b). Notably, EC-70124 treatment did not cause loss of weight (Fig. 3c) or other adverse effects. Histological examination of tumors showed that EC-70124-treated tumors exhibited lower mitotic counts and a significant reduction in tumor grade in comparison to untreated tumor samples (Figs. 3d and 3e).

The pharmacodynamic profile of EC-70124 was obtained by analyzing protein levels in tumors collected at different time-points in a subcohort of mice ( $n = 2-3$ ) upon a single 80 mg/kg dose (Fig. 3f). Pharmacodynamic effect of EC-70124 was in agreement with the results obtained in cultured cells. Thus, a partial inhibition of the phosphorylation of S6 and AKT was detected in tumor tissues 4 hr after the treatment, thus suggesting that same pathways identified *in vitro* are mediating the effects *in vivo* (Fig. 3f). Recovery profile of the proteins analyzed showed that the inhibition of the phosphorylation of the mTOR target S6 was sustained for at least 24–48 hr after dosing, while phospho-AKT showed a faster recovery (Fig. 3f).

#### **EC-70124 inhibits the expression and activity of ABC transporters and is not a substrate for them**

Several ABC transporters, such as ABCG2/BCRP1 and ABCB1/MDR1, play major roles in drug resistance in tumor cells.<sup>6–8</sup> It has been previously reported that a panel of indolocarbazole protein kinase inhibitors, including midostaurin, were able to inhibit the transport activity of ABCG2.<sup>39,40</sup> Therefore, we studied the interaction of EC-70124 with the two members of the ABC family most commonly involved in drug resistance of cancer cells. In functional assays, we found that EC-70124 efficiently inhibited the pumping activity of both ABCG2 and ABCB1 (Fig. 4a, Supporting Information Tables S4 and S5) and moreover, these pumps failed to transport this indolocarbazole analog (Fig. 4b and Supporting Information Table S6). Importantly, EC-70124 was also able to decrease the mRNA (Fig. 4c) and protein (Fig. 4d) expression of ABCG2 and ABCB1 in several MSC-5H and T-5H cell lines.

This inhibitory effect of EC-70124 on the expression and activity of ABC transporters suggest that, besides its antitumor activity, this drug may also play a role in counteracting drug resistance.

#### **EC-70124 and doxorubicin shows synergistic cytotoxic effect *in vitro* and *in vivo***

Doxorubicin-based therapies are still widely used as first-line treatments of both soft tissue and bone sarcomas.<sup>5</sup> However, doxorubicin, like many other chemotherapeutic agents, is a well-known substrate of ABC transporters.<sup>41</sup> Therefore, given the ability of EC-70124 to inhibit ABC transporters, we tested whether its combination with doxorubicin may produce a synergistic antitumor effect. First, we found that all sarcoma models were also sensitive to nanomolar concentrations of doxorubicin (IC<sub>50</sub> values between 74 and 318 nM; Supporting

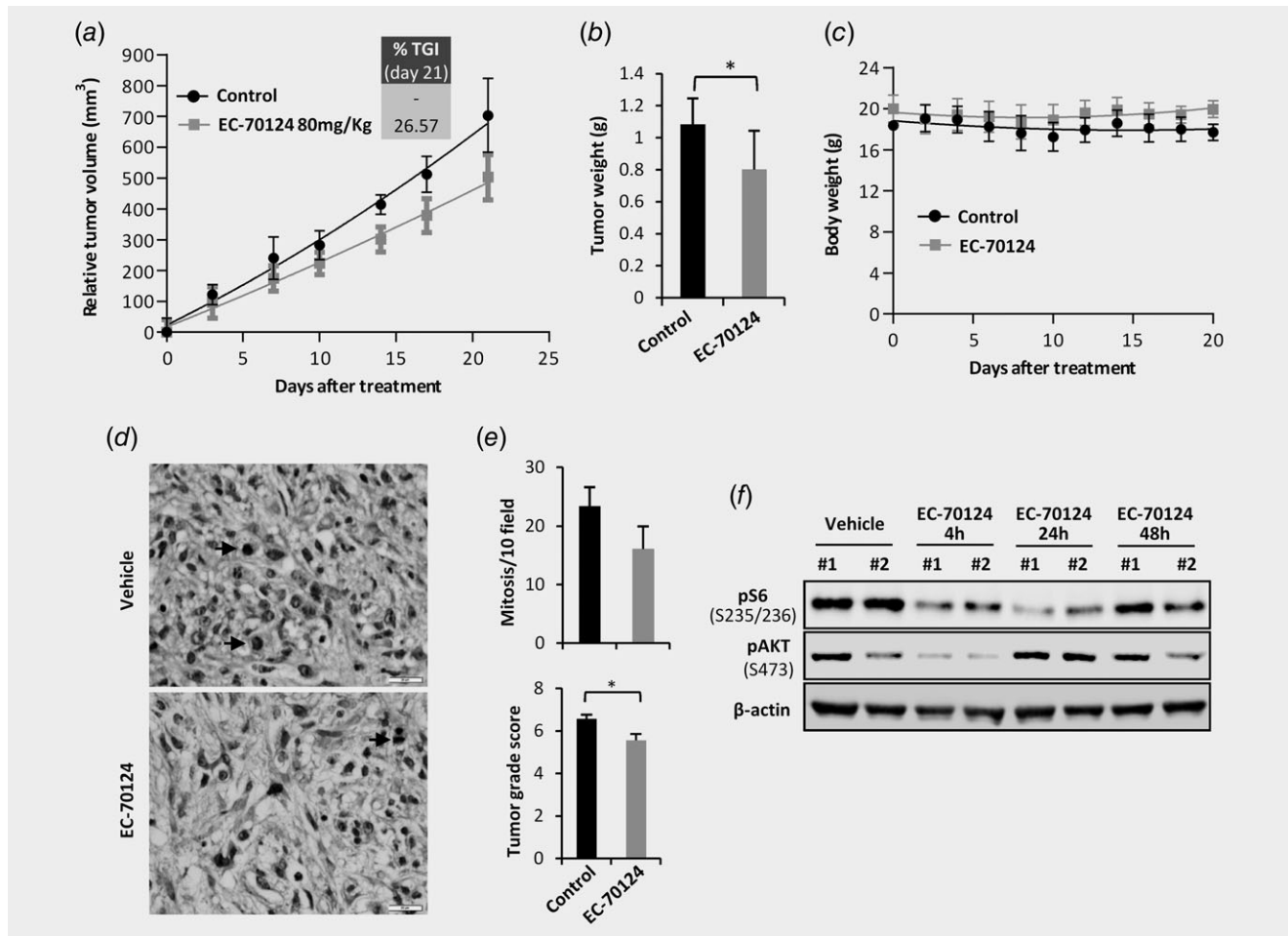


**Figure 3.** *In vivo* antitumor activity of EC-70124. NOD/SCID mice with established T-5H-FC#1 tumor xenografts were randomly assigned to three different groups ( $n = 7$  per group) and treated by oral gavage with either vehicle or EC-70124 at 80 mg/kg every 2 days. (a) Curves representing the mean tumor volume of T-5H-FC#1 xenografts during the treatments. Drug efficacy expressed as the percentage of TGI at day 21 is indicated. (b) Tumor weight at the end of the experiment. (c) Body weights of mice during the treatments. (d and e) Pathological analysis of formalin-fixed paraffin embedded xenografts extracted from mice treated as in panel a. (d) Representative images of the H&E staining of control and EC-70124-treated tumors. Mitotic cells (red arrows) are indicated. Scale bars = 50 μm. (e) Quantification of mitosis (number of mitotic figures per 10 high power fields [40X]) and tumor grade score according to FNCLCC system in tumors from the indicated series. (f) Intratumor phosphorylation levels (Western blotting analysis) of the key targets in samples collected at the indicated time points from mice treated with a single oral dose of 80 mg/kg EC-70124. Error bars represent the SEM and asterisks indicate statistically significant differences between EC-70124-treated and control groups (\* $p < 0.05$ ; two-sided Student *t* test).

Information Fig. S8). Doxorubicin treatment resulted in an up-regulation of phospho-S6, phospho-4EBP and ABCB1, while EC-70124, alone or in combination with doxorubicin efficiently decreased the levels of these targets (Fig. 5a). Importantly, the combination of EC-70124 with 100 nM doxorubicin significantly shifted toxicity curves and markedly decreased the IC<sub>50</sub> of EC-70124 in several sarcoma model cell lines but not in wild-type hMSCs (Fig. 5b). By calculating the CI of several constant ration combinations of EC-70124 and doxorubicin, we confirmed the existence of synergism between both drugs in MSC-5H-FC (CI value for ED<sub>75</sub> = 0.30) and T-5H-FC#1 cells (CI value for ED<sub>75</sub> = 0.62; Fig. 5c).

*In vivo* activity of the combination was evaluated in T-5H-FC#1 xenografts treated with oral doses of 40 mg/kg EC-70124

every 2 days and/or intravenous doses of 4 mg/kg doxorubicin every 4 days. By measuring the evolution of tumor volumes during the treatment (Fig. 6a) and tumor weights at the end of the experiments (Fig. 6b), we found that, as previously showed, EC-70124 caused certain level of tumor growth inhibition (% TGI = 27.2), whereas doxorubicin was more efficient in inhibiting tumor growth (% TGI = 68.7). Importantly, the combination of EC-70124 and doxorubicin was able to reduce tumor volumes (% TGI = 93.7) in a nearly statistically significant fashion ( $p = 0.09$ ) and tumor weights in a significant manner ( $p = 0.01$ ) compared to the effect of both drugs alone (Figs. 6a and 6b). Of note, mice treated with regimens including doxorubicin experienced important weight loss and the experiment had to be suspended on day 14 (Fig. 6c).

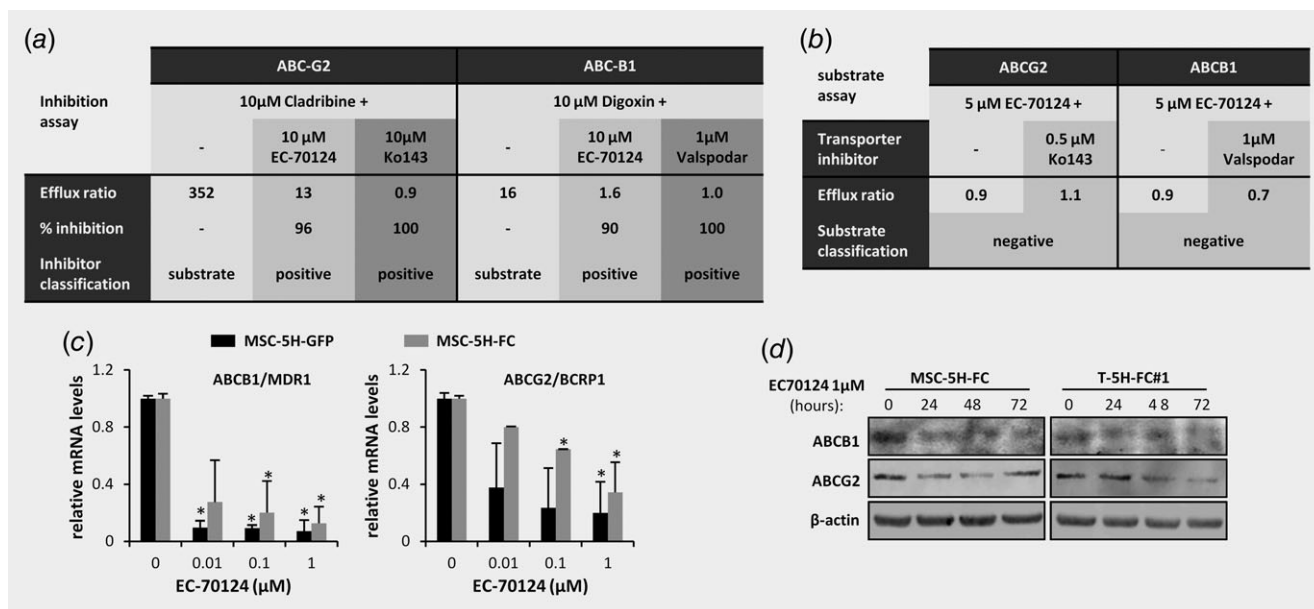


**Figure 4.** Effect of EC-70124 on ABC transporters expression and activity. (a) ABCG2 and ABCB1 functional inhibition assay for EC-70124. Cladribine and digoxin were used as known substrates and Ko243 and valsopodar were used as known inhibitors for ABCG2 and ABCB1, respectively. A complete summary of experimental results is shown in Supporting Information Tables S3 and S4. (b) ABCG2 and ABCB1 functional substrate assay for EC-70124. Ko243 and valsopodar were used as transporter inhibitors for ABCG2 and ABCB1, respectively. A complete summary of experimental results is shown in Supporting Information Table S5. (c) Relative mRNA expression of ABCG2 and ABCB1 genes in MSC-5H-GFP and MSC-5H-FC cells treated with the indicated concentrations of EC-70124 for 24 hr. Error bars represents the standard deviation of three independent experiments and asterisks indicate a statistically significant difference with the respective untreated samples (\* $p < 0.05$ ; two-sided Student  $t$  test). (d) Western blotting analysis of ABCG2, ABCB1 and  $\beta$ -actin after the indicated treatments with EC-70124.

Pharmacodynamic analysis showed that EC-70124 was able to inhibit the phosphorylation of S6 and AKT even in the presence of doxorubicin, which increased the phosphorylation of S6 in individual treatments (Fig. 6d). In addition, a notably increase in apoptosis (PARP cleavage) was detected in tumors treated with the combination (Fig. 6d). Histological examination confirmed the inhibition of phospho-S6, in tumors treated with EC-70124 alone or in combination with doxorubicin (Figs. 6e and 6f). In addition, tumors treated with doxorubicin alone or in combination with EC-70124 exhibited significantly reduced mitotic counts and tumor grade (Figs. 6e and 6f).

Altogether, these results indicate that the combination of EC-70124 and doxorubicin has a synergistic antitumor effect on sarcoma.

## Discussion

Indolocarbazole alkaloids have attracted great attention because of their original structural features and their ability to inhibit a wide spectrum of receptor and intracellular signaling kinases.<sup>25,42</sup> Among these compounds, midostaurin have been recently approved for the treatment of AML patients harboring mutations in FLT3.<sup>43</sup> In sarcoma, this drug has been found to inhibit the transcriptional activity of fusion oncogenes characteristic of alveolar rhabdomyosarcoma (PAX3/FKHR) and Ewing sarcoma (EWS/FLI1) as well as exhibited antitumor potential in these and other types of sarcoma.<sup>31–33</sup>

In addition, midostaurin has been shown to synergize with antitumor agents like HDAC inhibitors, oncostatin M or IGF1R inhibitors in different types of sarcoma.<sup>44,45</sup>

Here, we found that the indolocarbazole analog EC-70124 is much more efficient than midostaurin in inhibiting the phosphorylation of ERK1/2 at Thr202 and Tyr204, AKT at Ser473 and Thr308, pS6 at Ser235 and Ser236 and 4EBP at Ser65, which are the kinases/kinase substrates more activated among a panel of relevant signaling molecules in a cell-of-origin model of MRCLS. In a similar way, EC-70124 has recently demonstrated a higher capacity than midostaurin to inhibit several clinically relevant kinases in preclinical models of AML.<sup>29</sup> In addition, EC-70124 was also able to inhibit the activation of SRC, STAT1 and STAT3 which were found activated in several primary sarcoma cell lines. This higher potential of EC-70124 as multikinase inhibitor in sarcomas correlated with a more potent antiproliferative effect in comparison with midostaurin and the basis of this enhanced toxicity relies on the induction of much higher levels of DNA damage followed by a more stringent S-phase arrest and apoptosis. It has been reported that midostaurin and other indolocarbazoles inhibit Aurora kinase, resulting in abrogation of the mitotic spindle checkpoint and the accumulation of cells with 4 N and 8 N DNA content.<sup>46,47</sup> Here, we observed a similar effect after the treatment of sarcoma cells with midostaurin, although this endoreplication effect is not sufficient to

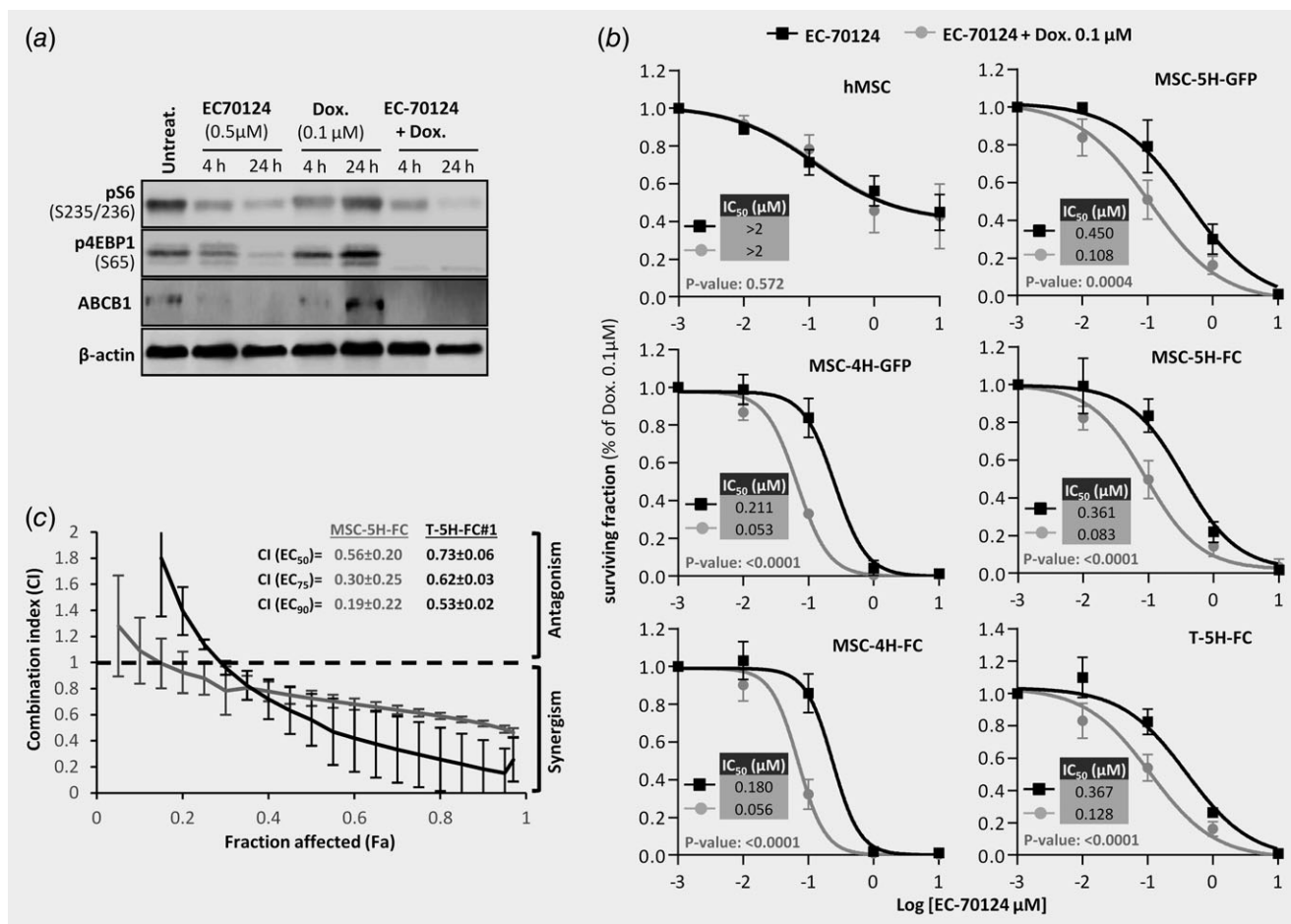


**Figure 5.** EC-70124 and doxorubicin shows synergistic cytotoxic effect. (a) Western blotting analysis of the indicated proteins after the indicated treatments with EC-70124 and/or doxorubicin. (b) Cell viability curves representing the IC<sub>50</sub> shift observed after 48 hr treatments of the indicated cell lines with EC70124 alone or in combination with 0.1 μM doxorubicin. Error bars represents the standard deviation of three independent experiments. (c) Combination index plots (mean and standard deviation) for constant ratio combinations of EC-70124 and doxorubicin (1:1) in MSC-5H-FC and T-5H-FC cells generated using the CompuSyn software. The CI (±standard deviation) values for ED<sub>50</sub>, ED<sub>75</sub> and ED<sub>90</sub> combination doses as calculated by the median effect equation are shown.

efficiently reduce cell viability. *In vitro* kinase binding affinity assays showed that EC-70124 inhibited Aurora kinases even more potently than midostaurin (Supporting Information Table S3) and opposite to this drug, EC-70124 was also a powerful inhibitor of CHK1, which is a key player in the sensing and the response to DNA damage in the S and G<sub>2</sub> phases of cell cycle.<sup>48</sup> This differential ability of both drugs to inhibit CHK1 may be responsible for the pronounced S-phase arrest and the increased DNA damage and apoptosis observed after the treatment with EC-70124 but not with midostaurin.

Downstream mTORC1 effectors S6 and 4EBP were the targets whose phosphorylation levels were more consistently inhibited by EC-70124 in all the sarcomas cell lines tested. The efficient inhibition of the phosphorylation of S6 correlates with the high affinity (low K<sub>d</sub>) of EC-70124 for S6K1 (Supporting Information Table S3). This data are in line with previously reported activity of EC-70124 in breast and colon cancer.<sup>27,30</sup> By combining EC-70124 or midostaurin with the

mTOR inhibitor torin, we studied the role of mTOR signaling in the cytotoxic effect of indolocarbazole analogs. Torin induced certain level of toxicity and did not synergize with EC-70124, which was an efficient mTOR inhibitor by itself and therefore did not allow for a mechanistic synergy with torin. On the other hand, torin synergized with midostaurin, which was a poor and transient inhibitor of mTOR signaling. Altogether, these results suggest that, although the inhibition of other targets could contribute, the blocking of mTOR signaling plays a key role in EC-70124-induced antiproliferative effects.

Despite the relevant role that PI3K/AKT/mTOR pathway plays in the pathogenesis of several types of sarcomas, including MRCLS,<sup>14–16</sup> and the promising antitumor activity observed *in vitro*, EC-70124 showed only a small, although significant, effect *in vivo*. This effect was accompanied with a partial and durable inhibition of phospho-S6 and a transient inhibition of phospho-AKT (S473) which recovered pretreatment levels after

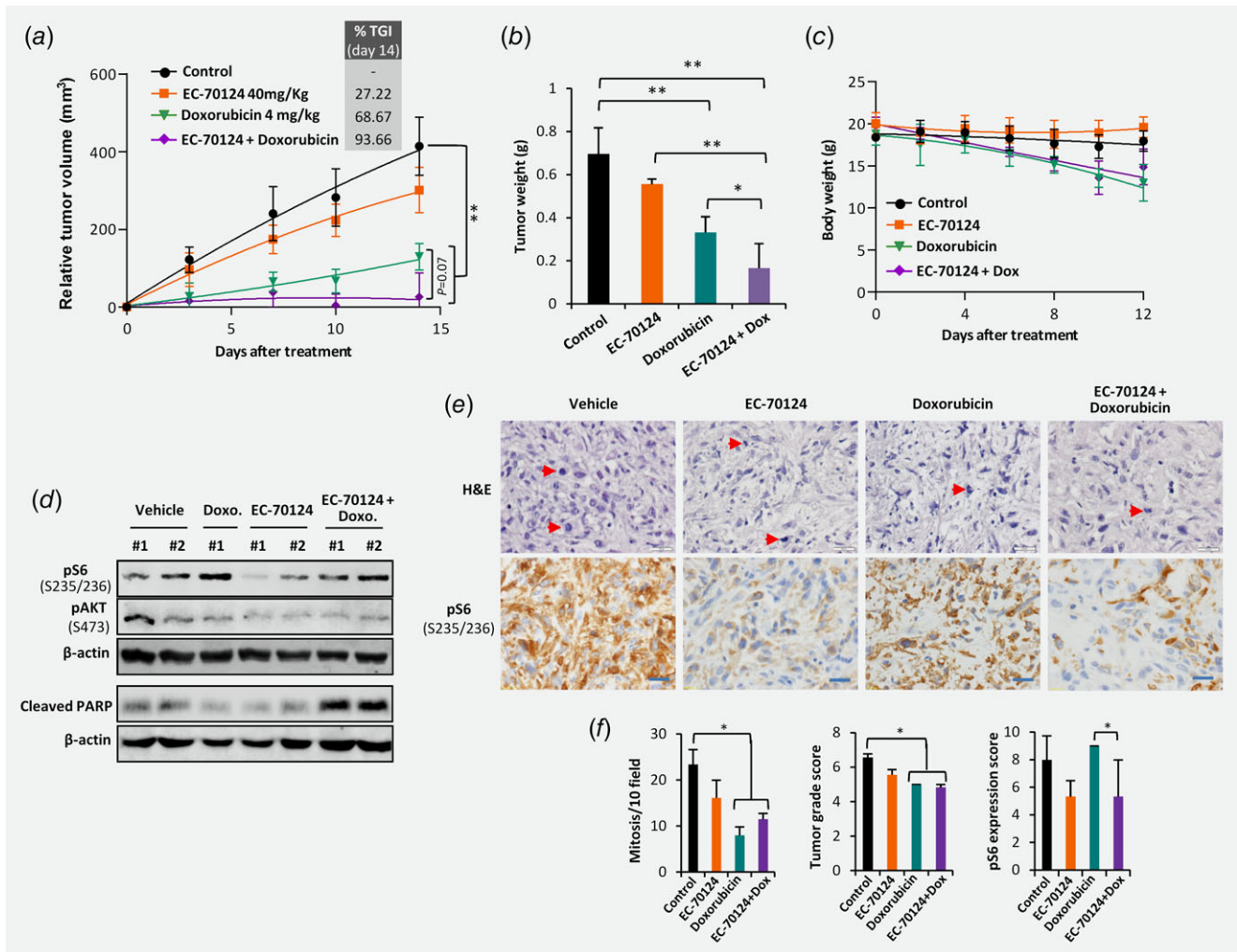


**Figure 6.** *In vivo* effect of EC-70124 and doxorubicin combination. T-5H-FC#1 established xenografts were randomly assigned to four different groups ( $n = 7$  per group) and treated with vehicle(s), with EC-70124 (orally) at a dose of 40 mg/kg every 2 days, with doxorubicin (intravenous) at a dose of 4 mg/kg on days 0, 4 and 8, or with a combination of both drugs. (a) Curves representing the mean tumor volume of T-5H-FC#1 xenografts during the treatments. Drug efficacy expressed as the percentage of TGI at day 14 is indicated. (b) Tumor weight at the end of the experiment. (c) Body weights of mice during the treatments. (d) Intratumor phosphorylation levels (Western blotting analysis) of the key targets in samples collected after 0 and 4 hr of a single dose of the previously described treatments. (e and f) Pathological analysis of formalin-fixed paraffin embedded xenografts extracted from mice treated as in panel a. (e) H&E staining and immuno-staining detection of phospho-S6. Mitotic cells (red arrows) are indicated. Scale bars = 50  $\mu$ m. (f) Quantification of tumor related features including mitosis (number of mitotic figures per 10 high power fields [40 $\times$ ]) and tumor grade score according to FNCLCC system and levels of phospho-S6 (number of cell showing positive staining per 10 high power fields [40 $\times$ ]) in tumors from the indicated series. Error bars represent the SEM and asterisks indicate statistically significant differences between groups. Extra sum-of-squares  $F$  test were used in panel a and two-sided Student  $t$  test were used in panels b, d and f ( $*p < 0.05$ ;  $**p < 0.01$ ). [Color figure can be viewed at [wileyonlinelibrary.com](http://wileyonlinelibrary.com)]

24 hr. Several mechanisms of resistance involving the recovering of PI3K/AKT signaling after the activation of mTORC2 *via* IGF1R or PDGFR signaling have been described for different mTOR inhibitors.<sup>20,22,23</sup> Therefore, the restoring of AKT signaling may be in the basis of the resistance to the treatment with EC-70124. Nevertheless, we have not detected an increased phosphorylation of IGF1R or PDGFR after EC-70124-treatment *in vitro* (Supporting Information Fig. S4), thus suggesting that other unknown mechanisms may be mediating the reactivation of AKT.

Signaling mediated by PI3K-AKT-mTOR has been involved in drug resistance in a wide range of tumors.<sup>9,19</sup> Accordingly, mTOR inhibitors were able to restore sensitivity against tyrosin kinase inhibitors and chemotherapeutic drugs like doxorubicin, cisplatin or paclitaxel in several types of tumors including sarcomas.<sup>9,19,49</sup> Apart from the antiapoptotic and pro-survival signals mediated by PI3K-AKT-mTOR signaling, the upregulation of members of ABC family of transporters through the activation of this pathway seems to be another important mechanism of drug resistance.<sup>19,50</sup> In these

regard, several Indolocarbazoles have demonstrated its ability to inhibit ABCB1 and/or ABCG2 and reverse drug resistance.<sup>39,40</sup> In addition, several tyrosine kinase inhibitors have been recently reported to increase the efficacy of conventional chemotherapeutic agents through mechanisms involving the inhibition and/or the expression of different ABC pumps.<sup>8</sup> Here, we found that EC-70124 was able to inhibit the enzymatic activity and the expression of ABCB1 and ABCG2 and moreover, it was not transported by these pumps. In line with this result, we showed that the combination of EC-70124 with doxorubicin produced a synergistic decrease of cell viability and a reduction in tumor growth *in vivo*. These findings suggest that the ability of EC-70124 to inhibit ABC transporters maybe in the basis of these enhanced antitumor potential of the combination.

Altogether, these results uncover the capability of the novel multikinase inhibitor EC-70124 to counteract drug resistance in sarcoma and provide a rationale for the clinical testing of the EC-70124 plus doxorubicin combination in sarcoma patients.

## References

1. Abarrategi A, Tornin J, Martinez-Cruzado L, et al. Osteosarcoma: cells-of-origin, cancer stem cells, and targeted therapies. *Stem Cells Int* 2016; 2016:1–13.
2. Rodriguez R, Rubio R, Menendez P. Modeling sarcomagenesis using multipotent mesenchymal stem cells. *Cell Res* 2012;22:62–77.
3. Chen C, Borker R, Ewing J, et al. Epidemiology, treatment patterns, and outcomes of metastatic soft tissue sarcoma in a community-based oncology network. *Sarcoma* 2014;2014:145764.
4. Martinez-Cruzado L, Tornin J, Rodriguez A, et al. Trabectedin and Camptothecin synergistically eliminate cancer stem cells in cell-of-origin sarcoma models. *Neoplasia* 2017;19:460–70.
5. Ratan R, Patel SR. Chemotherapy for soft tissue sarcoma. *Cancer* 2016;122:2952–60.
6. Szakacs G, Paterson JK, Ludwig JA, et al. Targeting multidrug resistance in cancer. *Nat Rev Drug Discov* 2006;5:219–34.
7. Bugde P, Biswas R, Merien F, et al. The therapeutic potential of targeting ABC transporters to combat multi-drug resistance. *Expert Opin Ther Targets* 2017;21:511–30.
8. Wu S, Fu L. Tyrosine kinase inhibitors enhanced the efficacy of conventional chemotherapeutic agent in multidrug resistant cancer cells. *Mol Cancer* 2018;17:25.
9. Blay JY. Updating progress in sarcoma therapy with mTOR inhibitors. *Ann Oncol* 2011;22:280–7.
10. Dobashi Y, Suzuki S, Sato E, et al. EGFR-dependent and independent activation of Akt/mTOR cascade in bone and soft tissue tumors. *Mod Pathol* 2009;22:1328–40.
11. Saxton RA, Sabatini DM. mTOR signaling in growth, metabolism, and disease. *Cell* 2017;168:960–76.
12. Setsu N, Kohashi K, Fushimi F, et al. Prognostic impact of the activation status of the Akt/mTOR pathway in synovial sarcoma. *Cancer* 2013;119:3504–13.
13. Barretina J, Taylor BS, Banerji S, et al. Subtype-specific genomic alterations define new targets for soft-tissue sarcoma therapy. *Nat Genet* 2010;42:715–21.
14. Demicco EG, Torres KE, Ghadimi MP, et al. Involvement of the PI3K/Akt pathway in myxoid/round cell liposarcoma. *Mod Pathol* 2012; 25:212–21.
15. Patel RB, Li T, Liao Z, et al. Recent translational research into targeted therapy for liposarcoma. *Stem Cell Investig* 2017;4:21.
16. Sanfilippo R, Dei Tos AP, Casali PG. Myxoid liposarcoma and the mammalian target of rapamycin pathway. *Curr Opin Oncol* 2013;25:379–83.
17. Tornin J, Hermida-Prado F, Padda RS, et al. FUS-CHOP promotes invasion in myxoid liposarcoma through a SRC/FAK/RHO/ROCK-dependent pathway. *Neoplasia* 2018;20:44–56.
18. Trautmann M, Menzel J, Bertling C, et al. FUS-DDIT3 fusion protein-driven IGF-IR signaling is a therapeutic target in myxoid liposarcoma. *Clin Cancer Res* 2017;23:6227–38.
19. Jiang BH, Liu LZ. Role of mTOR in anticancer drug resistance: perspectives for improved drug treatment. *Drug Resist Updat* 2008;11:63–76.
20. Ho AL, Vasudeva SD, Lae M, et al. PDGF receptor alpha is an alternative mediator of rapamycin-induced Akt activation: implications for combination targeted therapy of synovial sarcoma. *Cancer Res* 2012;72:4515–25.
21. Mita MM, Gong J, Chawla SP. Ridaforolimus in advanced or metastatic soft tissue and bone sarcomas. *Expert Rev Clin Pharmacol* 2013;6:465–82.
22. Lamhamedi-Cherradi SE, Menegaz BA, Ramamoorthy V, et al. IGF-1R and mTOR blockade: novel resistance mechanisms and synergistic drug combinations for Ewing sarcoma. *J Natl Cancer Inst* 2016;108:djw182.
23. May CD, Landers SM, Bolshakov S, et al. Co-targeting PI3K, mTOR, and IGF1R with small molecule inhibitors for treating undifferentiated pleomorphic sarcoma. *Cancer Biol Ther* 2017;18:816–26.
24. Slotkin EK, Patwardhan PP, Vasudeva SD, et al. MLN0128, an ATP-competitive mTOR kinase inhibitor with potent *in vitro* and *in vivo* antitumor activity, as potential therapy for bone and soft-tissue sarcoma. *Mol Cancer Ther* 2015;14:395–406.
25. Sanchez C, Salas AP, Brana AF, et al. Generation of potent and selective kinase inhibitors by combinatorial biosynthesis of glycosylated indolocarbazoles. *Chem Commun (Camb)* 2009;27:4118–20.
26. Civenni G, Longoni N, Costales P, et al. EC-70124, a novel glycosylated Indolocarbazole multi-kinase inhibitor, reverts tumorigenic and stem cell properties in prostate cancer by inhibiting STAT3 and NF-kappaB. *Mol Cancer Ther* 2016;15:806–18.
27. Cuenca-Lopez MD, Serrano-Heras G, Montero JC, et al. Antitumor activity of the novel multi-kinase inhibitor EC-70124 in triple negative breast cancer. *Oncotarget* 2015;6:27923–37.
28. Nogueira L, Ruiz-Ontanon P, Vazquez-Barquero A, et al. Blockade of the NFkappaB pathway drives differentiating glioblastoma-initiating cells into senescence both *in vitro* and *in vivo*. *Oncogene* 2011;30:3537–48.
29. Puente-Moncada N, Costales P, Antolin I, et al. Inhibition of Flt3 and Pim kinases by EC-70124 exerts potent activity in preclinical models of acute myeloid leukemia. *Mol Cancer Ther* 2018; 17:614–24.
30. Serrano-Heras G, Cuenca-Lopez MD, Montero JC, et al. Phospho-kinase profile of colorectal tumors guides in the selection of multi-kinase inhibitors. *Oncotarget* 2015;6:31272–83.
31. Amstutz R, Wachtel M, Troxler H, et al. Phosphorylation regulates transcriptional activity of PAX3/FKHR and reveals novel therapeutic possibilities. *Cancer Res* 2008;68:3767–76.

32. Boro A, Pretre K, Rechfeld F, et al. Small-molecule screen identifies modulators of EWS/FLI1 target gene expression and cell survival in Ewing's sarcoma. *Int J Cancer* 2012; 131:2153–64.
33. Kawamoto T, Akisue T, Kishimoto K, et al. Inhibition of PKC $\alpha$  activation in human bone and soft tissue sarcoma cells by the selective PKC inhibitor PKC412. *Anticancer Res* 2008;28:825–32.
34. Rodriguez R, Rosu-Myles M, Arauzo-Bravo M, et al. Human bone marrow stromal cells lose immunosuppressive and anti-inflammatory properties upon oncogenic transformation. *Stem Cell Rep* 2014;3:606–19.
35. Rodriguez R, Tornin J, Suarez C, et al. Expression of FUS-CHOP fusion protein in immortalized/-transformed human mesenchymal stem cells drives mixoid liposarcoma formation. *Stem Cells* 2013;31:2061–72.
36. Martinez-Cruzado L, Tornin J, Santos L, et al. Aldh1 expression and activity increase during tumor evolution in sarcoma cancer stem cell populations. *Sci Rep* 2016;6:27878.
37. Tornin J, Martinez-Cruzado L, Santos L, et al. Inhibition of SP1 by the mithramycin analog EC-8042 efficiently targets tumor initiating cells in sarcoma. *Oncotarget* 2016;7:30935–50.
38. Rubio R, Abarrategi A, Garcia-Castro J, et al. Bone environment is essential for osteosarcoma development from transformed mesenchymal stem cells. *Stem Cells* 2014;32:1136–48.
39. Robey RW, Shukla S, Steadman K, et al. Inhibition of ABCG2-mediated transport by protein kinase inhibitors with a bisindolylmaleimide or indolocarbazole structure. *Mol Cancer Ther* 2007; 6:1877–85.
40. Utz I, Hofer S, Regenass U, et al. The protein kinase C inhibitor CGP 41251, a staurosporine derivative with antitumor activity reverses multidrug resistance. *Int J Cancer* 1994;57: 104–10.
41. Wu D, Liu L, Yan X, et al. Pleiotrophin promotes chemoresistance to doxorubicin in osteosarcoma by upregulating P-glycoprotein. *Oncotarget* 2017; 8:63857–70.
42. Gallogly MM, Lazarus HM. Midostaurin: an emerging treatment for acute myeloid leukemia patients. *J Blood Med* 2016;7:73–83.
43. Manley PW, Weisberg E, Sattler M, et al. Midostaurin, a natural product-derived kinase inhibitor recently approved for the treatment of hematological malignancies published as part of the biochemistry series "biochemistry to bedside". *Biochemistry* 2018;57:477–8.
44. Brounais B, Chipoy C, Mori K, et al. Oncostatin M induces bone loss and sensitizes rat osteosarcoma to the antitumor effect of midostaurin in vivo. *Clin Cancer Res* 2008;14:5400–9.
45. Radic-Sarikas B, Tsafou KP, Emdal KB, et al. Combinatorial drug screening identifies Ewing sarcoma-specific sensitivities. *Mol Cancer Ther* 2017;16:88–101.
46. Kawai M, Nakashima A, Kamada S, et al. Midostaurin preferentially attenuates proliferation of triple-negative breast cancer cell lines through inhibition of Aurora kinase family. *J Biomed Sci* 2015;22:48.
47. Stolz A, Vogel C, Schneider V, et al. Pharmacologic abrogation of the mitotic spindle checkpoint by an indolocarbazole discovered by cellular screening efficiently kills cancer cells. *Cancer Res* 2009;69:3874–83.
48. Rodriguez R, Gagou ME, Meuth M. Apoptosis induced by replication inhibitors in Chk1-depleted cells is dependent upon the helicase cofactor Cdc45. *Cell Death Differ* 2008;15: 889–98.
49. Squillace RM, Miller D, Cookson M, et al. Antitumor activity of ridaforolimus and potential cell-cycle determinants of sensitivity in sarcoma and endometrial cancer models. *Mol Cancer Ther* 2011;10:1959–68.
50. Lee JT Jr, Steelman LS, McCubrey JA. Phosphatidylinositol 3'-kinase activation leads to multidrug resistance protein-1 expression and subsequent chemoresistance in advanced prostate cancer cells. *Cancer Res* 2004;64:8397–404.